Published in final edited form as:
Nat Commun. ; 1: 3. doi:10.1038/ncomms1001.

Sirt1 improves healthy ageing and protects from metabolic syndrome-associated cancer syndrome

Daniel Herranz[1], **Marta Cañamero**[2], **Francisca Mulero**[3], **Barbara Martinez-Pastor**[4], **Oscar Fernandez-Capetillo**[4], and **Manuel Serrano**[1,*]

[1]Tumor Suppression Group, Spanish National Cancer Research Center (CNIO) Madrid, Spain

[2]Comparative Pathology Unit, Spanish National Cancer Research Center (CNIO) Madrid, Spain

[3]Molecular Imaging Unit, Spanish National Cancer Research Center (CNIO) Madrid, Spain

[4]Genomic Instability Group Spanish National Cancer Research Center (CNIO) Madrid, Spain

Abstract

Genetic overexpression of the protein deacetylase Sir2 increases longevity in a variety of lower organisms, and this has prompted a great interest on the effects of its closest mammalian homologue, Sirt1, on aging and cancer. We have generated transgenic mice moderately overexpressing Sirt1 under its own regulatory elements (Sirt1-tg). Old Sirt1-tg mice present lower levels of DNA damage, decreased expression of the aging-associated gene p16Ink4a, a better general health and fewer spontaneous carcinomas and sarcomas. These effects, however, were not sufficiently potent to affect longevity. To further extend these observations, we developed a metabolic syndrome-associated liver cancer model in which wild-type mice develop multiple carcinomas. Sirt1-tg mice show a reduced susceptibility to liver cancer and exhibited improved hepatic protection from both DNA damage and metabolic damage. Together, these results provide direct proof for the anti-aging activity of Sirt1 in mammals and for its tumour suppression activity in aging- and metabolic syndrome-associated cancer.

Overexpression of the protein deacetylase Sir2 in yeasts, flies and worms has the remarkable effect of extending longevity [1,2]. Mammals have evolved a family of Sir2-related proteins known as sirtuins and composed by seven members (Sirt1-7), of which Sirt1 is the closest homologue to Sir2 [2]. However, little is known at present about the impact of mammalian Sirt1 on aging [3]. Regarding cancer, available genetic evidence supports a tumor suppressor role of Sirt1 [4]. In particular, decreased Sirt1 activity accelerated the tumor-prone phenotype of p53-heterozygous mice [5] and, reciprocally, overexpression of Sirt1 in lymphocytes delayed the development of radiation-induced lymphomas in p53-heterozygous mice [6]. Moreover, Sirt1 binds and deacetylates β-catenin, thus canceling its oncogenic transcriptional activity and decreasing intestinal tumor development [7]. While the above results are of obvious importance, it remains to be determined the impact of systemic Sirt1 upregulation on aging and on aging-associated cancer. This is particularly relevant given the ongoing efforts to develop drugs that stimulate Sirt1 activity, including resveratrol and

[*]*Correspondence*: Spanish National Cancer Research Center (CNIO) 3 Melchor Fernandez Almagro street Madrid E-28029, Spain Tel.: +34.91.732.8000 Fax: +34.91.732.8033 mserrano@cnio.es.

AUTHOR CONTRIBUTIONS D.H. performed most of the experiments, contributed to data analysis, discussion and writing the manuscript; M.C. performed all the pathological analyses; F.M. performed all the imaging analysis by microCT; B.M.-P. performed the DNA repair assays; O.F.-C. designed and supervised the DNA damage data; M.S. designed and supervised the study, secured funding, analyzed the data, and wrote the manuscript. All authors discussed the results and commented on the manuscript.

The authors declare no competing financial interests with this paper.

Europe PMC Funders Author Manuscripts

SRT1720 [8-10]. Regarding these latter compounds, it is controversial whether they activate Sirt1 directly [8,9,11,12]. Alternatively, resveratrol may upregulate Sirt1 through indirect mechanisms that could involve AMPK [13,14].

It has been previously reported by others and us that transgenic mice systemically overexpressing Sirt1 (~3-fold) are protected from the physiological damage produced by high-fat diet (HFD) [15,16]. These observations are further reinforced by the phenotype of mice deficient in Dbc1, a negative regulator of Sirt1, and which also show systemic activation of Sirt1 and protection from HFD-induced damage [17]. At a molecular level, protection against HFD has been reported to reflect the activity of Sirt1 as a negative regulator of NFκB [15,17] and as a positive effector of PGC1α [15] and FoxO1 [16]. Chronic exposure to high levels of dietary fat results in a multi-systemic deterioration known as metabolic syndrome and characterized by insulin resistance, liver steatosis, atherogenic cardiovascular disease, dyslipidaemia, and systemic inflammation, which may lead to fatal diseases such as liver cancer and heart failure [18,19]. Given the prevalence of metabolic syndrome in the adult and aged human population [20], it is of interest to determine the impact of Sirt1 upregulation on metabolic syndrome-associated cancer.

Here, we examine the aging and longevity of the Sirt1-tg mice, as well as, their susceptibility to spontaneous cancer and to liver cancer associated to metabolic syndrome. Our results indicate that Sirt1 exerts anti-aging activity in mammals, although this effect is not sufficiently potent to extend longevity, at least at the levels of overexpression achieved in our mice. Sirt1-tg mice are protected from the development of aging-associated diseases such as glucose intolerance, osteoporosis and cancer. Moreover, Sirt1 provides a strong protection against liver cancer development in a context of metabolic syndrome.

RESULTS

Normal longevity and decreased spontaneous cancer

To evaluate the impact of Sirt1 on mammalian aging, we have analyzed two independent lines of Sirt1 transgenic mice carrying different, but overlapping, genomic DNA segments (**Supplementary Fig. S1a**). These two lines, named here as Sirt1-tgA [15] and Sirt1-tgB, overexpress ~3-fold Sirt1 mRNA across all the tissues tested (**Supplementary Fig. S1b**), and present detectably higher levels of Sirt1 protein (**Supplementary Fig. S2a-c**), as well as, an increase in hepatic Sirt1 activity measured by the lower levels of acetylated lysine 310 of p65RelA (**Supplementary Fig. S2c**), a known target of Sirt1 deacetylase activity [21]. In agreement with their similar levels of Sirt1 upregulation, Sirt1-tgB mice display the same phenotypes previously reported by us for Sirt1-tgA mice [15], namely, protection from HFD-induced adipose tissue inflammation (**Supplementary Fig. S3a**), glucose intolerance (**Supplementary Fig. S3b**), and hepatic steatosis (**Supplementary Fig. S3c**), as well as, increased sensitivity to lypopolysaccharide shock under standard diet (**Supplementary Fig. S4**).

To determine the impact of Sirt1 upregulation on longevity we followed cohorts of the two lines together with their corresponding wt controls. All cohorts had the same uniform but hybrid genetic background (C57BL6/CBA 87.5%:12.5%). The corresponding survival curves are represented either separating the two lines or pooling them together. Pooling allowed us to achieve a cohort size per genotype and sex of n>40, which provides sufficient statistical power to reliably detect differences greater than 10% in mean lifespan [22]. The survival curves of Sirt1-tg(A+B) and wt(A+B) were indistinguishable for both males and females (Fig. 1a). When males and females were put together the number of mice wt and tg mice was n>100 and, again, no differences were detected in survival (Fig. 1a). Moreover, no significant differences were found between Sirt1-tg lines and their corresponding wt controls

(Fig. 1a). We conclude that systemic 3x-fold upregulation of Sirt1 has no detectable impact, neither detrimental nor beneficial, on mouse longevity. Detailed histopathological analyses of old moribund mice revealed a lower incidence of malignant tumors in Sirt1-tg mice, compared to wt mice of both lines (Fig. 1b). Remarkably, the suppressive effect of Sirt1 on malignant tumors was restricted to carcinomas and sarcomas (mostly osteosarcomas), while it had no effect on the incidence of lymphomas and histiocytic lymphomas (the latter also known as histiocytic sarcomas) (Fig. 1c). It is important to mention that most spontaneous carcinomas and sarcomas were in general of small size (as was the case of liver or lung carcinomas) or affected non-vital organs (such as Harderian gland carcinomas in the eyes or osteosarcomas in the limbs). Therefore, despite their malignancy, most of these cancers were at a stage of dissemination that is unlikely to be the primary cause of death. This is in contrast to spontaneous lymphomas, which had similar incidences in wt and tg mice, and were highly aggressive and the likely cause of death. In summary, these results indicate that Sirt1 upregulation provides protection from spontaneous carcinomas and sarcomas, but not from spontaneous lymphomas.

Improved healthy aging

To examine the impact of Sirt1 on aging, we began by examining a physiological parameter related to the metabolic syndrome, namely aging-associated glucose intolerance [23]. Young (3 months old) wt and Sirt1-tg mice under standard diet showed similar performance in glucose-tolerance tests (GTT) [15,16] (see also **Supplementary Fig. S3b**). Interestingly, at 1.5 years of age, wt mice already showed evidence of glucose intolerance, while transgenic Sirt1 mice preserved a significantly better glucose uptake (Fig. 2a). These results indicate that Sirt1 confers protection from aging-associated metabolic damage under standard diet and, together with previous data on mice under high-fat diet [15-17], reinforce and extend the concept that Sirt1 is a general protector from metabolic damage. Another common feature of aging is the development of osteoporosis, a process that can be promoted by NFκB [24,25] whose activity is increased during aging [26]. In agreement with the reported ability of Sirt1 to inhibit NFκB [15,17,21], we observed that Sirt1-tg mice preserved normal bone density values at old age (2.5 years), while wt mice showed a significant decline in bone density at this age (Fig. 2b). Additional indicators of fitness at old age were obtained by measuring skin regeneration (wound healing assay, Fig. 2c) and neuromuscular coordination (tightrope assay, Fig. 2d), both of which suggested a better performance by Sirt1-tgA mice (no effect at this level was detected in Sirt1-tgB mice). To evaluate aging at a molecular level, we measured two well-established markers of aging, namely, the levels of $p16^{Ink4a}$ mRNA [27] and the accumulation of nuclear foci of DNA damage proteins [28,29]. In the case of $p16^{Ink4a}$, its transcript levels in liver increased >15-fold in old wt mice compared to young ones (2 years *vs.* 3 months), while this increase was significantly attenuated to ~7-fold in Sirt1-tg animals (Fig. 2e). Moreover, the number of cells with 53BP1 DNA damage foci in the liver was reduced in old Sirt1-tg compared to wt mice of the same age (Fig. 2f). Collectively, the analysis of aging-associated pathologies (glucose intolerance, osteoporosis, decreased wound-healing, impaired neuromuscular coordination) and molecular markers of aging ($p16^{Ink4a}$, DNA damage) support the concept that Sirt1 possess anti-aging activity in mammals.

Decreased metabolic syndrome-associated liver cancer

After analyzing the effect of Sirt1 on health and cancer during aging, we wanted to further extend the cancer studies to a model relevant for metabolic syndrome, a condition that affects up to one quarter of the human population after middle age [19,20]. The array of diseases comprised by metabolic syndrome can be initiated by a high dietary intake and, in the particular case of the liver, it results in fatty liver, followed by cirrhosis and, finally, cancer [18,30]. To model metabolic syndrome-associated cancer, we treated mice with a single

injection of a hepatic-specific carcinogen, diethylnitrosamine (DEN), followed by continued exposure to HFD. To decrease inter-individual variation due to the hybrid genetic background, all the following assays were performed in mice that had been backcrossed for 8 generations with C57BL6 mice and therefore were >99% C57BL6. Also, it is relevant to note that DEN is a poor carcinogen on its own in mice of the C57BL6 genetic background [31]. In fact, most of our wt mice (6/11 = 55%) were completely free of liver tumors at 11 months post-treatment with DEN under standard diet conditions. Importantly, all the wt mice treated with DEN and under HFD for 11 months developed multiple tumors (on average 10 tumors) that were quantified and measured in live mice by micro-computed tomography (microCT) (Fig. 3a). Notably, the corresponding Sirt1-tg littermate mice presented a significantly lower incidence and burden of liver tumors (Fig. 3a). Upon necropsy, the differences in tumor number and size between wt and Sirt1-tg livers were dramatic (Fig. 3b) and histological analyses confirmed that all the tumors, both in wt and tg mice, correspond to liver carcinomas (Fig. 3c). We wondered whether the strong protection observed against DEN/HFD-induced hepatocarcinogenesis was also present in other protocols of chemical carcinogenesis. However, when we induced fibrosarcomas with 3-methyl-cholanthrene (3MC), no differences were observed between wt and Sirt1-tg mice (Fig. 3d). This differential cancer protection between hepatocytes and fibroblasts, correlated with the impact of Sirt1 on DNA damage in the same cell types (see below). We conclude that moderate upregulation of Sirt1 strongly suppresses metabolic syndrome-associated liver cancer.

Hepatic protection from carcinogenic damage

Sirt1-tg mice present a lower accumulation of aging-associated DNA damage in liver (see above Fig. 2f), and other investigators have found that Sirt1 contributes to maintain genomic stability [5,6]. Based on these observations, it can be hypothesized that Sirt1-mediated protection from DEN/HFD-induced liver cancer reflects a dual impact of Sirt1, decreasing the damage produced both by DEN and HFD. While the protection of Sirt1 from HFD-induced damage is well substantiated [15-17] (see also **Supplementary Fig. S3**), nothing is known about the impact of Sirt1 on DEN-induced liver damage. Treatment of mice with DEN under standard feeding conditions triggers a well-known cascade of events in the liver that include DNA damage and apoptosis of centrolobular hepatocytes, production of pro-inflammatory cytokines, and compensatory proliferation [32]. Serum levels of alanine transaminase (ALT) 48 h after DEN injection already indicated a significant protection from liver injury in Sirt1-tg mice in standard diet (Fig. 4a). Immunohistological examination of livers 48 h post-DEN showed intense nuclear staining of Sirt1 restricted to the centrolobular regions of the liver (around the central veins, CV) and absent in the periportal regions (around the portal triad, PT) (Fig. 4b and panoramic views in **Supplementary Fig. S5a**). Treatment of *in vitro* cultured cells with genotoxic agents recruits Sirt1 to the chromatin [6], and we wondered whether this was also happening *in vivo* upon DEN. Indeed, we observed that DEN increased the amount of chromatin-bound Sirt1 in liver extracts, without detectably affecting the total amount of Sirt1 (Fig. 4c). After observing that Sirt1 is actively responding to DEN by concentrating in the nucleus and stably binding to chromatin, we examined the impact of Sirt1-tg on the liver upon treatment with DEN under standard feeding conditions. Livers from wt mice showed a strong DNA damage response in the centrolobular regions accompanied by high levels of apoptosis and compensatory proliferation (Fig. 4d and panoramic views in **Supplementary Fig. S5b**). Importantly, and in sharp contrast, DEN-treated Sirt1-tg livers showed significantly lower levels of damage, apoptosis and compensatory proliferation (Fig. 4d and panoramic views in **Supplementary Fig. S5b**). DEN is known to require bioactivation by cytochrome CYP2E1 [33], and we asked whether Sirt1 could be exerting its protective effect by directly affecting DEN metabolism. To address this question, we measured CYP2E1 mRNA levels in control or DEN-treated

livers. DEN-treatment decreased CYP2E1 levels as previously reported [34], but no differences in its levels could be observed between wt and Sirt1-tg mice, thus suggesting that Sirt1 is not affecting DEN bioactivation (Fig. 4e). Next, we wondered whether Sirt1 protection against DNA damage was also detectable in fibroblasts, however, detailed kinetic analyses of γH2AX in individual cells upon treatment with neocarzinostatin could not detect a better repair in Sirt1-tg compared to wt fibroblasts (**Supplementary Fig. S6**). Our assays suggest a cell type specificity in the effects of Sirt1 on DNA damage, being more protective in hepatocytes than in fibroblasts. However, the assays and DNA damage agents used here preclude a direct comparison and this point remains to be clarified in future studies. Therefore, overexpression of Sirt1 at the levels achieved in our mouse lines (3x-fold) significantly protect hepatocytes, but not fibroblasts, from DNA damage, and this correlates with a strong protection against DEN/HFD-induced liver carcinoma but not against 3MC-induced fibrosarcomas (see above Fig. 3).

DISCUSSION

In this work, we provide direct genetic evidence for the anti-aging activity of Sirt1 in mammals. We have found that moderate upregulation of Sirt1 expression (3x-fold) improves healthy aging but not longevity. Importantly, old Sirt1-tg mice are partially protected from the development of pathologies typically associated to aging, like glucose intolerance, osteoporosis, or poor wound healing. This improved maintenance of physiological fitness at old ages is accompanied by a decreased expression of molecular markers of aging in liver, particularly $p16^{Ink4a}$ mRNA levels and DNA damaged cells. However, the overall impact on aging under standard *ad libitum* feeding conditions was not sufficiently potent to extend longevity. Given the beneficial impact of Sirt1 on aging, it is tempting to speculate that attaining levels of Sirt1 activity higher than those achieved by us, either genetically or through the use of pharmacological activators, could lead to lifespan extension. Moreover, taking into account that there are seven different sirtuins in mammalian organisms, it is also possible that several sirtuins must be targeted concurrently to produce lifespan extension. An important observation derived from the analyses of old moribund Sirt1-tg mice is that they are partially protected from spontaneous carcinomas and sarcomas, but not from lymphomas. Other investigators have reported that Sirt1 protects from lymphomas in p53-heterozygous mice [5,6]. It is conceivable that Sirt1 has a stronger protective effect against lymphomas with a high degree of genetic instability, such as those developed in p53-heterozygous mice. Whereas, spontaneous lymphomas develop less aggressively late in life and are presumably less dependent on protection from acute DNA damage. In the case of spontaneous carcinomas, it is possible that Sirt1 could exert its protective effect both through preventing DNA damage, but also through deacetylation and inhibition of β-catenin [7], which is an oncogene generally associated to epithelial cancers [35]. Together, these factors could explain, at least in part, the differential effect of Sirt1 on aging-associated carcinomas and sarcomas, *versus* lymphomas.

Caloric restriction (CR) is a well-known manipulation with the ability to delay aging and increase lifespan [36]. It has been proposed that the beneficial effects of CR in mice are mediated, at least in part, through Sirt1 [37-39]. In this regard it is interesting to note that our Sirt1-tg mice present an improved glucose tolerance at old ages, which is a characteristic feature of CR-treated mice [40]. Further studies are necessary to address the similarities between Sirt1-tg mice under *ad libitum* conditions and CR-treated mice. In this context, it is also worth to point out the similarities between the phenotypes of our Sirt-tg mice and the reported effects of the small natural compound resveratrol on mice, which upregulates Sirt1 activity, perhaps indirectly through effects mediated by AMPK[13,14]. Mice chronically fed with resveratrol are protected from metabolic syndrome induced by high-fat diet [13,41] and present an improved healthy aging without affecting longevity [42]. Interestingly, whereas

resveratrol did not protect from spontaneous cancers [42], our Sirt1-tg mice were partially protected from these cancers.

The role of Sirt1 in protection from metabolic syndrome is solidly established [15-17]. Based on this, we have developed a novel carcinogenic protocol to model metabolic syndrome-associated cancer. Metabolic syndrome leads over time to liver steatosis, followed by cirrhosis, which, in turn, is the main risk factor for the development of liver carcinoma [18,30]. Specifically, this new experimental cancer model consists on a single injection of the hepatic-specific carcinogen diethylnitrosamine (DEN), followed by continued exposure to high-fat diet. This protocol produced a 100% incidence of liver carcinomas in wild-type C57BL6 mice. Importantly, Sirt1-tg littermate mice were dramatically protected. We show here that the resistance to liver cancer in Sirt1-tg mice is due to a dual protective effect both from the initial acute damage elicited by the carcinogen (DEN), as well as, from the chronic damage produced by the high-fat diet. In agreement with previous reports implicating Sirt1 in the maintenance of genomic stability [5,6], we demonstrate here that Sirt1-tg mice are protected from DEN-triggered DNA damage in hepatocytes *in vivo*. These results reinforce the association between metabolic syndrome and liver cancer, and demonstrate the critical role of Sirt1 in protection from these pathologies. In this context, it is of relevance to mention that recent analyses of Sirt1 expression in a wide variety of human cancers has found decreased Sirt1 expression in liver cancer, but not in most other human malignancies [5]. Together, our observations demonstrate that chronic and systemic upregulation of Sirt1 is beneficial for health and cancer.

Note added in proof

A similar liver cancer mouse model initiated by diethylnitrosamine (DEN) and promoted by high-fat diet has been reported while this work was under consideration (Park, E. J., Lee, J. H., Yu, G.-Y., He, G., Ali, S. R., Holzer, R. G., Osterreicher, C. H., Takahashi, H. & Karin, M. *Cell* **140**, 197-208 (2010)).

METHODS

Animal Experimentation

The Sirt1-tgB line was generated following the same protocol described for the generation of Sirt1-tgA line [15]. Both BACs were obtained from CHORI (identification numbers: RP23-119G23 for tgA line and RP24-306L15 for tgB line) and purified using the Large-Construct kit (Quiagen). For transgenesis, the Sirt1-containing BACs were digested with the restriction enzyme PI-SceI, thus linearizing them in the vector at a position adjacent to the T7 end of the genomic inserts. Pronuclei of fertilized oocytes, derived from intercrosses between (C57BL6 × CBA)F1 mice, were injected with ~2 pl of a DNA solution (~1 ng/ml) containing the linearized BACs. The resulting offspring was analyzed for the presence of the transgenes using PCR reactions that amplify sequences from each vector (primers tgA-F 5′-agatagttcaccggggtgagaa-3′; tgA-R 5′-ttcggtcgaagagtatctggtg-3′; tgB-F 5′-actctttaaccggcccttacaag-3′; tgB-R 5′-tcctgtggatctacccactagtca-3′).

All mice were housed at the serum pathogen free (SPF) barrier area of the Spanish National Cancer Research Center (CNIO), Madrid. Mice were treated in accordance with the Spanish Laws and the Guidelines for Human Endpoints for Animals Used in Biomedical Research. Mice were observed on a daily basis and sacrificed when they showed signs of morbidity or overt tumors. The genetic background of the mice used in the aging assays was 87.5% C57BL6 and 12.5% CBA (after 2 backcrosses). For the rest of the experiments, >99% C57BL6 (after 8 backcrosses) mice were used. Mice were fed either with a standard chow

Europe PMC Funders Author Manuscripts

diet (Teklad 2018), or with a high-fat diet (Research Diets 12451, 45% kJ from fat) when indicated.

For the glucose tolerance test (GTT), wt and tg mice on both diets were subjected to 6 h of fasting and injected intraperitoneally (i.p.) with 2 g/kg glucose, and glucose levels in serum were determined using Glucocard strips (A. Meranini Diagnostics). For the wound-healing assay, wounds were made in the back skin using 4 mm biopsy punches, and healing was measured after 48 h by two researchers blind to the experiment, with the following semiquantitative scoring: 0 for well healed, dry and almost closed wounds; 2 for moist and overtly opened wounds; and 1 for intermediate ones. Osteoporosis was assessed in femurs of living mice on a microCT system (eXplore Vista PET/CT, GEHC), analyzing the values obtained from the scans acquired with 150 mAmp, 45 KVolt, 360 projections, 8 shots and 200 μm of resolution. BMD and HU measurements were obtained using Microwave Software ABA (Advanced Bone Analysis) selecting an area of interest from the femur. For the neuromuscular coordination assay (tightrope), mice were placed on a bar of circular section (60 cm long and 1.5 cm diameter) and the test was considered successful when a mouse stayed on the bar more than 60 sec throughout five consecutive trials. For the short time response to DEN studies, 100 mg/kg DEN (Sigma) was injected i.p. to < 4-month-old males. To determine proliferation, 100 mg/kg BrdU (Sigma) was injected i.p. 2 h prior to sacrifice. ALT levels in serum were determined using VetScan® Comprehensive Diagnostic Profile rotors (Abaxis).

Mouse Tumor Models

For the DEN/HFD-tumorigenesis model, 16-day-old males were injected with 5 mg/kg DEN, and then fed on a HFD (see above) since weaning. Tumor detection and measurement was performed by microCT in living mice as described for the osteoporosis measurements except that, in this case, mice were intravenously injected with the iodinated contrast agent Iopamiro 300 (Bracco). Tumor sizes were measured using eXplore Vista software.

For the 3MC-tumorigenesis model, 2-4 months old animals were injected intramuscularly in one of the rear legs with 1 mg of 3-methyl-cholanthrene (Sigma) dissolved in 100 μl of corn oil. Mice were observed on a daily basis and sacrificed when the tumors reached a diameter >1.5cm.

Quantitative RT-PCR

Total RNA from all tissues was extracted with Trizol (Invitrogen, Carlsbad, CA). Reverse transcription was performed using random priming and Superscript Reverse Transcriptase (Life Technologies). Quantitative real-time PCR was performed using DNA Master SYBR Green I mix (Applied Biosystems) in an ABI PRISM 7700 thermocycler (Applied Biosystems, Carlsbad, CA). Variations in input RNA were corrected by substracting the number of PCR cycles obtained for β-actin. Primer sequences are described in **Supplementary Table S1**.

Protein analyses

For isolation of hepatocytes, livers were collected and sliced into small pieces with surgical blades and then incubated at 37°C for 30 min with 2 mg/ml of collagenase (Stemcell Technologies) solution containing 10 mM HEPES, 136 mM NaCl, 5 mM KCl, 0.5% glucose, 0.7 mM $CaCl_2$, 1 mM of DTT and a cocktail of protease inhibitors. Hepatocytes where then filtered trough a 70μm cell-strainer (BD). To isolate the chromatin, hepatocytes where then resuspended in 200 μl of buffer containing 10 mM HEPES, 10 mM KCl, 1.5 mM $MgCl_2$, 0.34 M sucrose and 10% glycerol. Then, Triton-X-100 was added to 0.1%. Intact nuclei were spun down and resuspended in a buffer containing 3 mM EDTA and 0.2

mM EGTA, followed by incubation on ice for 30 min. The pellet obtained after spinning down these samples contained the isolated chromatin, which was resuspended in 1× Laemmli buffer. The following antibodies were used: anti-Sirt1 (ab12193, Abcam, 1:2000), anti-actin (AC-15, Sigma, 1:5000) and anti-H3 (ab1791, Abcam, 1:1000), anti-Ac(K310)-p65 (ab19870, Abcam, 1:200) and anti-p65 (sc-8008, Santa Cruz, 1:200).

Histological and immunohistochemical methods

Detailed histopathological analysis of aged moribund mice was performed by one of the authors (MC, a trained pathologist). Liver sections from DEN-treated mice were stained with the following antibodies: anti-Sirt1 (S5196, Sigma, 1:3000), anti-BrdU (BU-1, GE Healthcare, 1:100) or anti-γH2AX (JBW301, Millipore, 1:2000). For the TUNEL stainings, ApopTag Peroxidase In Situ Apoptosis Detection Kit was used (Millipore). DNA damage in aged livers was assessed by confocal immunofluorescence against 53BP1 (NB100-304, Novus Biologicals, 1:500) on paraffin-embedded sections. For quantifications of DNA damage (γH2AX), apoptosis (TUNEL) and compensatory proliferation (BrdU) in DEN-treated livers, at least 5 microscope fields at 20× magnification, and always containing a CV and a PT, were scored for positive cells ($n \geq 3$ per genotype). In all graphs, the values represented are relative to wt controls.

Statistical analyses

Kaplan-Meier curves were compared using the logrank test. Cancer incidences were compared using the Fisher's exact test. All the other measurements were compared using the two-tailed Student's t-test.

Acknowledgments

We are indebted to Maribel Muñoz and Gema Iglesias for excellent mouse handling. We thank Antonio Maraver and Pablo J. Fernández-Marcos for helpful discussions. D.H. is supported by a predoctoral fellowship from the Spanish Ministry of Health and by the "Francisco Cobos" Foundation. Work in the laboratory of M.S. is funded by the CNIO and by grants from the Spanish Ministry of Science (SAF and CONSOLIDER), the Regional Government of Madrid (GsSTEM), the European Union (PROTEOMAGE), the European Research Council (ERC Advanced Grant), and the "Marcelino Botin" Foundation. The funders had no role in study design, data collection and analysis, decision to publish, or preparation of the manuscript.

REFERENCES

1. Bishop NA, Guarente L. Genetic links between diet and lifespan: shared mechanisms from yeast to humans. Nat Rev Genet. 2007; 8:835–844. [PubMed: 17909538]
2. Michan S, Sinclair D. Sirtuins in mammals: insights into their biological function. Biochem J. 2007; 404:1–13. [PubMed: 17447894]
3. Garber K. A mid-life crisis for aging theory. Nat Biotechnol. 2008; 26:371–374. [PubMed: 18392009]
4. Deng CX. SIRT1, is it a tumor promoter or tumor suppressor? Int J Biol Sci. 2009; 5:147–152. [PubMed: 19173036]
5. Wang RH, et al. Impaired DNA damage response, genome instability, and tumorigenesis in SIRT1 mutant mice. Cancer Cell. 2008; 14:312–323. [PubMed: 18835033]
6. Oberdoerffer P, et al. SIRT1 redistribution on chromatin promotes genomic stability but alters gene expression during aging. Cell. 2008; 135:907–918. [PubMed: 19041753]
7. Firestein R, et al. The SIRT1 deacetylase suppresses intestinal tumorigenesis and colon cancer growth. PLoS One. 2008; 3:e2020. [PubMed: 18414679]
8. Howitz KT, et al. Small molecule activators of sirtuins extend Saccharomyces cerevisiae lifespan. Nature. 2003; 425:191–196. [PubMed: 12939617]
9. Milne JC, et al. Small molecule activators of SIRT1 as therapeutics for the treatment of type 2 diabetes. Nature. 2007; 450:712–716. [PubMed: 18046409]

10. Alcain FJ, Villalba JM. Sirtuin activators. Expert Opin Ther Pat. 2009; 19:403–414. [PubMed: 19441923]
11. Beher D, et al. Resveratrol is not a direct activator of SIRT1 enzyme activity. Chem Biol Drug Des. 2009; 74:619–624. [PubMed: 19843076]
12. Pacholec M, et al. SRT1720, SRT2183, SRT1460, and resveratrol are not direct activators of SIRT1. J Biol Chem. 2010 d.o.i. 10.1074/jbc.M109.088682.
13. Baur JA, et al. Resveratrol improves health and survival of mice on a high-calorie diet. Nature. 2006; 444:337–342. [PubMed: 17086191]
14. Canto C, et al. AMPK regulates energy expenditure by modulating NAD+ metabolism and SIRT1 activity. Nature. 2009; 458:1056–1060. [PubMed: 19262508]
15. Pfluger PT, Herranz D, Velasco-Miguel S, Serrano M, Tschop MH. Sirt1 protects against high-fat diet-induced metabolic damage. Proc Natl Acad Sci U S A. 2008; 105:9793–9798. [PubMed: 18599449]
16. Banks AS, et al. SirT1 gain of function increases energy efficiency and prevents diabetes in mice. Cell Metab. 2008; 8:333–341. [PubMed: 18840364]
17. Escande C, et al. Deleted in breast cancer-1 regulates SIRT1 activity and contributes to high-fat diet-induced liver steatosis in mice. J Clin Invest. 2010; 120:545–558. [PubMed: 20071779]
18. Watanabe S, Yaginuma R, Ikejima K, Miyazaki A. Liver diseases and metabolic syndrome. J Gastroenterol. 2008; 43:509–518. [PubMed: 18648737]
19. Huang PL. A comprehensive definition for metabolic syndrome. Dis Model Mech. 2009; 2:231–237. [PubMed: 19407331]
20. Luchsinger JA. A work in progress: the metabolic syndrome. Sci Aging Knowledge Environ. 2006; 2006:e19.
21. Yeung F, et al. Modulation of NF-kappaB-dependent transcription and cell survival by the SIRT1 deacetylase. Embo J. 2004; 23:2369–2380. [PubMed: 15152190]
22. Ladiges W, et al. Lifespan extension in genetically modified mice. Aging Cell. 2009
23. Guarente L. Sirtuins as potential targets for metabolic syndrome. Nature. 2006; 444:868–874. [PubMed: 17167475]
24. Ruocco MG, et al. I{kappa}B kinase (IKK){beta}, but not IKK{alpha}, is a critical mediator of osteoclast survival and is required for inflammation-induced bone loss. J Exp Med. 2005; 201:1677–1687. [PubMed: 15897281]
25. Chang J, et al. Inhibition of osteoblastic bone formation by nuclear factor-kappaB. Nat Med. 2009; 15:682–689. [PubMed: 19448637]
26. Adler AS, et al. Motif module map reveals enforcement of aging by continual NF-kappaB activity. Genes Dev. 2007; 21:3244–3257. [PubMed: 18055696]
27. Krishnamurthy J, et al. Ink4a/Arf expression is a biomarker of aging. J Clin Invest. 2004; 114:1299–1307. [PubMed: 15520862]
28. Sedelnikova OA, et al. Senescing human cells and ageing mice accumulate DNA lesions with unrepairable double-strand breaks. Nat Cell Biol. 2004; 6:168–170. [PubMed: 14755273]
29. Herbig U, Ferreira M, Condel L, Carey D, Sedivy JM. Cellular senescence in aging primates. Science. 2006; 311:1257. [PubMed: 16456035]
30. Powell EE, Jonsson JR, Clouston AD. Steatosis: co-factor in other liver diseases. Hepatology. 2005; 42:5–13. [PubMed: 15962320]
31. Sun D, et al. Inactivation of p27Kip1 promotes chemical mouse liver tumorigenesis in the resistant strain C57BL/6J. Mol Carcinog. 2008; 47:47–55. [PubMed: 17620307]
32. Maeda S, Kamata H, Luo JL, Leffert H, Karin M. IKKbeta couples hepatocyte death to cytokine-driven compensatory proliferation that promotes chemical hepatocarcinogenesis. Cell. 2005; 121:977–990. [PubMed: 15989949]
33. Kang JS, Wanibuchi H, Morimura K, Gonzalez FJ, Fukushima S. Role of CYP2E1 in diethylnitrosamine-induced hepatocarcinogenesis in vivo. Cancer Res. 2007; 67:11141–11146. [PubMed: 18056438]

34. Freeman JE, Stirling D, Russell AL, Wolf CR. cDNA sequence, deduced amino acid sequence, predicted gene structure and chemical regulation of mouse Cyp2e1. Biochem J. 1992; 281(Pt 3): 689–695. [PubMed: 1536649]

35. Polakis P. The many ways of Wnt in cancer. Curr Opin Genet Dev. 2007; 17:45–51. [PubMed: 17208432]

36. Guarente L, Picard F. Calorie restriction--the SIR2 connection. Cell. 2005; 120:473–482. [PubMed: 15734680]

37. Chen D, Steele AD, Lindquist S, Guarente L. Increase in activity during calorie restriction requires Sirt1. Science. 2005; 310:1641. [PubMed: 16339438]

38. Bordone L, et al. SIRT1 transgenic mice show phenotypes resembling calorie restriction. Aging Cell. 2007; 6:759–767. [PubMed: 17877786]

39. Boily G, et al. SirT1 regulates energy metabolism and response to caloric restriction in mice. PLoS One. 2008; 3:e1759. [PubMed: 18335035]

40. Hempenstall S, Picchio L, Mitchell SE, Speakman JR, Selman C. The impact of acute caloric restriction on the metabolic phenotype in male C57BL/6 and DBA/2 mice. Mech Ageing Dev. 2010; 131:111–118. [PubMed: 20064544]

41. Lagouge M, et al. Resveratrol improves mitochondrial function and protects against metabolic disease by activating SIRT1 and PGC-1alpha. Cell. 2006; 127:1109–1122. [PubMed: 17112576]

42. Pearson KJ, et al. Resveratrol delays age-related deterioration and mimics transcriptional aspects of dietary restriction without extending life span. Cell Metab. 2008; 8:157–168. [PubMed: 18599363]

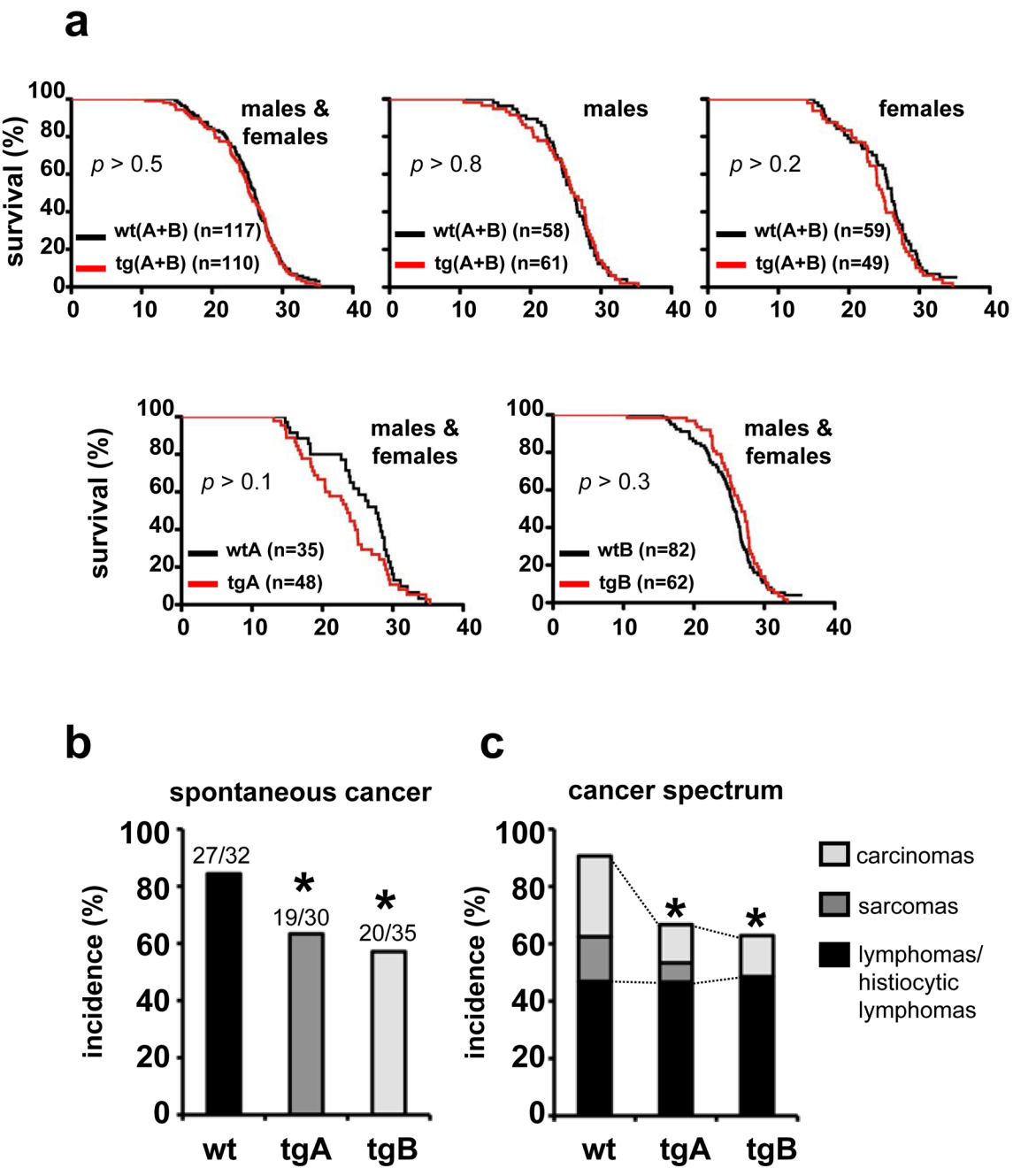

Figure 1. Normal lifespan but enhanced cancer protection in Sirt1-tg mice

(**a**) Survival of cohorts of mice of the indicated genotypes. Logrank tests indicated that Sirt1-tg mice were not statistically different from wt mice ($p > 0.05$). **(b)** Spontaneous cancer incidence. Statistical significance *vs* wt mice was calculated using the Fisher's Exact test : *$p < 0.05$. (**c**) Cancer spectrum. Statistical analysis refers to the combined incidence of carcinomas and sarcomas *vs* wt mice using the Fisher's Exact test : *$p < 0.05$.

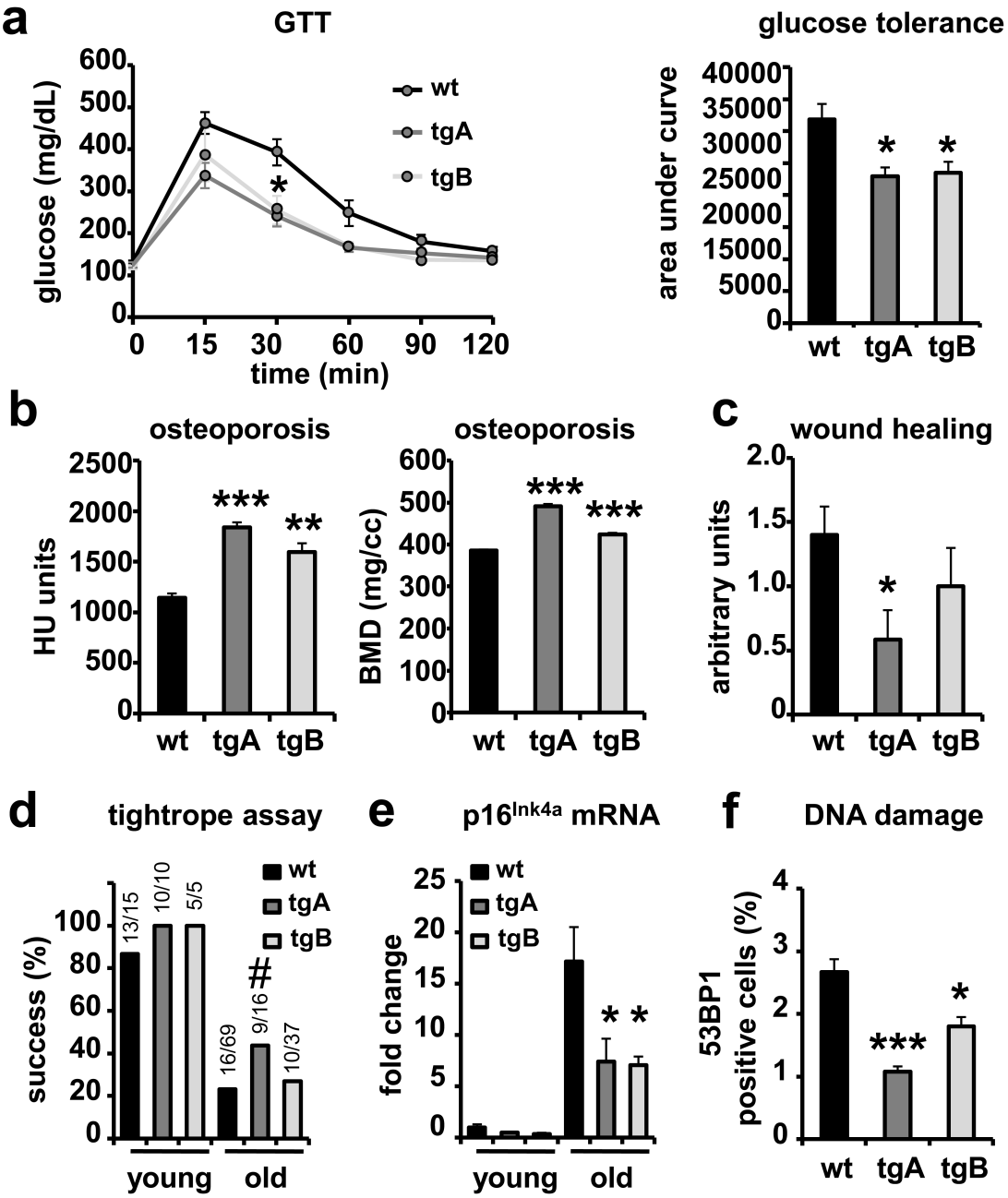

Figure 2. Improved healthy aging in Sirt1-tg mice

(**a**) Glucose tolerance test in 1.5 years old male mice (n ≥ 4 per group). Curves are shown to the left. Integrated AUCs (area under curve) are shown to the right. (**b**) Osteoporosis was analyzed in 2.5 years old male mice (n = 3 per group) by microcomputed tomography (microCT). Values of Hounsfield units (HU) and bone mineral density (BMD) for the entire femurs are shown. (**c**) Wound-healing assay in ≥ 2 years old mice (n ≥ 10 per group). (**d**) Neuromuscular coordination assay. Young (< 6 months) and old (> 2 years) mice were subjected to the tightrope assay. (**e**) Levels of $p16^{Ink4a}$ mRNA in livers of young (< 6 months) and old (≥ 2 years) mice (n ≥ 3 per group) were analyzed by qRT-PCR. Data are

relative to the levels in young wt mice. (**f**) Levels of DNA damage in the liver of old (≥ 2 years) mice (n ≥ 3 per genotype) measured as the percentage of 53BP1-foci positive nuclei by confocal microscopy. In all graphs except panel (d), values are given as average ± SEM, and statistical analyses are relative to wt controls and determined by the two-tailed Student's t-test: *$p < 0.05$; **$p < 0.01$; ***$p < 0.005$. For panel (d), statistical significance was calculated using the Fisher's Exact test: #$p < 0.1$.

Europe PMC Funders Author Manuscripts

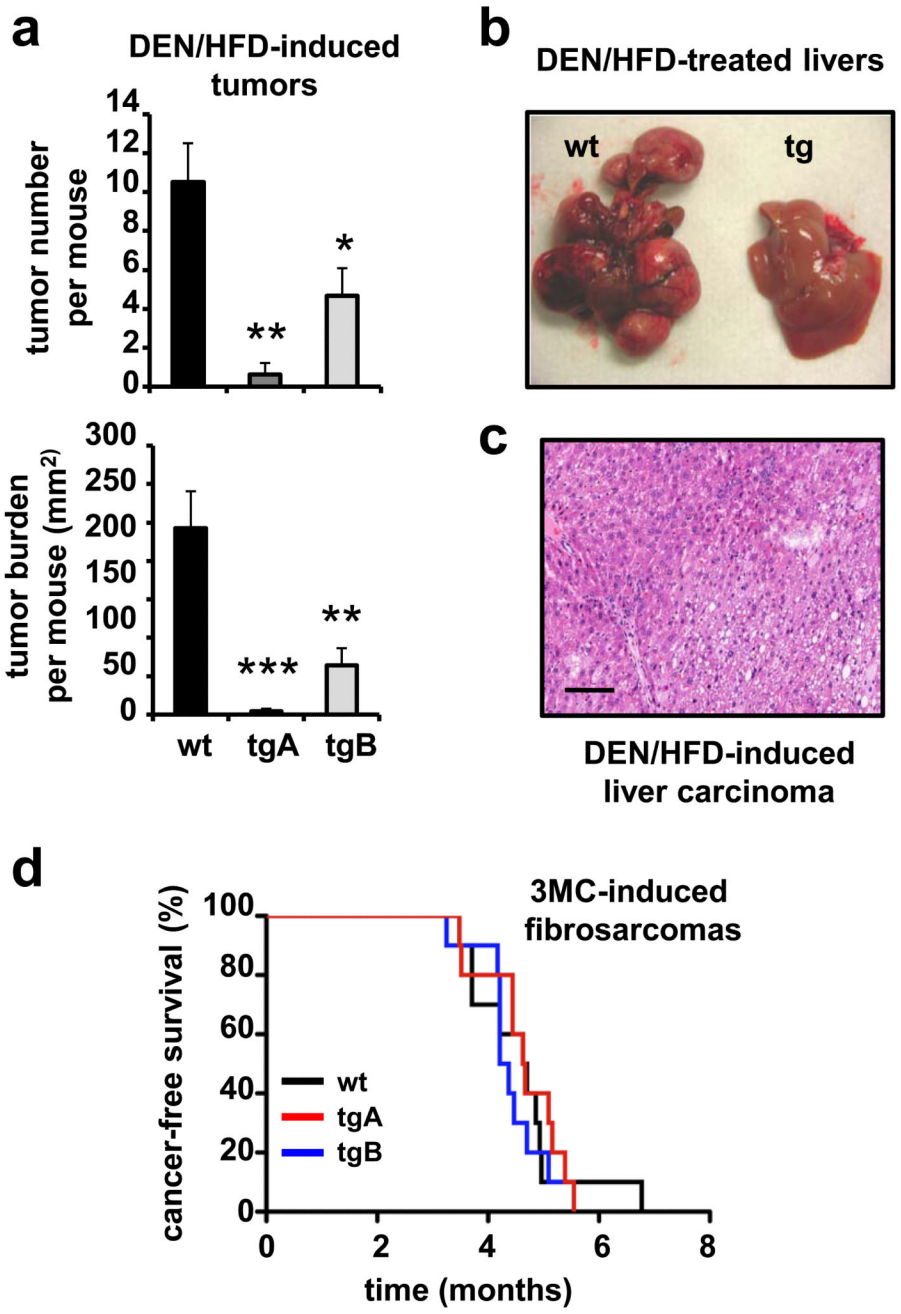

Figure 3. Sirt1 protects from metabolic syndrome-associated liver cancer

(**a**) Tumor number and tumor burden in mice injected with diethylnitrosamine (DEN) and maintained for 11 months under high-fat diet (HFD). Tumors were measured by microCT. Tumor burden per mouse was obtained by adding the areas of the biggest section of each tumor. All the assays were performed with male mice (n ≥ 5 per group). Values are given as average ± SEM, statistical analyses are relative to wt controls and determined by the two-tailed Student's t-test: *$p < 0.05$; **$p < 0.01$; ***$p < 0.005$. (**b**) Macroscopic view of representative livers from littermate mice of the indicated genotypes 11 months after initiation of the DEN/HFD protocol. (**c**) Histology of a representative liver carcinoma

induced by the DEN/HFD protocol. Hematoxylin and eosin staining. The bar indicates 100 μm. (**d**) Susceptibility to 3MC-induced fibrosarcomas. Mice of the indicated genotypes were injected intramuscularly with 3-methyl-cholanthrene (3MC) in one of the rear legs and the latency for the development of fibrosarcomas was scored. Logrank test indicated no significant differences ($p > 0.6$) between genotypes.

Europe PMC Funders Author Manuscripts

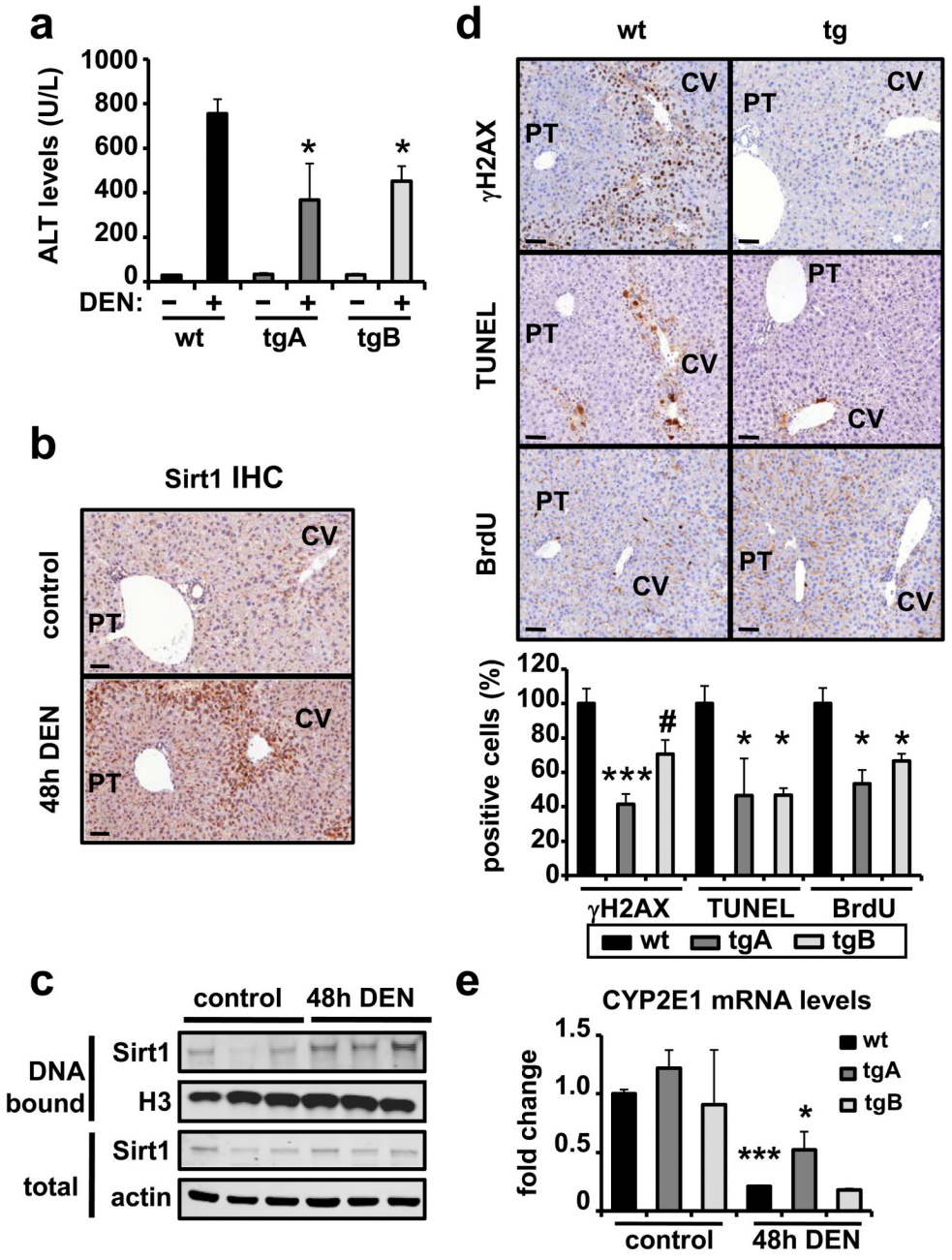

Figure 4. Sirt1 protects from DNA damage in the liver

(**a**) Alanine transaminase (ALT) levels in serum before or 48 hours after DEN injection (n ≥ 3 per group). (**b**) Liver sections stained for Sirt1 before or 48 hours after DEN injection in wt mice. The bar indicates 50 μm. (**c**) Liver protein levels of Sirt1 bound to chromatin or in total extracts from wt mice (n=3) before or 48 hours after DEN injection. Histone H3 and actin were used as loading controls. (**d**) Representative stainings of DNA damage (γH2AX), apoptosis (TUNEL), and compensatory proliferation (BrdU), each showing a centrolobular area (around a centrolobular vein marked as CV) and a portal area (around a portal triad marked as PT) of livers of mice 48 hours after DEN injection. Bars indicate 50 μm.

Europe PMC Funders Author Manuscripts

Quantifications are shown below relative to wt DEN-treated livers. For quantifications, at least 5 microscope fields at 20× magnification, always containing a CV and a PT were scored (n ≥ 3 per genotype). (**e**) Levels of CYP2E1 in the livers of control or DEN-treated mice (n ≥ 3 per group). Differences between tg samples and wt control were not significant ($p > 0.1$) in all cases. In all graphs, values are given as average ± SEM, statistical analyses are relative to wt controls and determined by the two-tailed Student's t-test: #$p < 0.1$; *$p < 0.05$; ***$p < 0.005$.

Europe PMC Funders Author Manuscripts